

A Beam Monitor Using Silicon Pixel Sensors for Hadron Therapy

Zhen Wang, Shuguang Zou, Yan Fan, Jun Liu, Xiangming Sun*, Dong Wang, Huili Kang, Daming Sun, Ping Yang, Hua Pei, Guangming Huang, Nu Xu, Chaosong Gao, Le Xiao

^aPLAC, Key Laboratory of Quark & Lepton Physics (MOE), Central China Normal University, Wuhan, Hubei 430079, P.R.China

Abstract

We report the design and test results of a beam monitor developed for online monitoring in hadron therapy. The beam monitor uses eight silicon pixel sensors, *Topmetal-II*⁻, as the anode array. *Topmetal-II*⁻ is a charge sensor designed in a CMOS 0.35 μm technology. Each *Topmetal-II*⁻ sensor has 72×72 pixels. Each pixel size is about $83 \times 83 \mu\text{m}^2$. In our design the beam passes through the beam monitor without hitting the electrodes, making the beam monitor especially suitable for monitoring heavy ion beams. This design also reduces radiation damage to the beam monitor itself. The beam monitor is tested at the Heavy Ion Research Facility in Lanzhou (HIRFL) which provides a carbon ion beam. Results indicate that the beam monitor can measure position, incident angle and intensity of the beam with a position resolution better than 20 μm , angular resolution about 0.5° and intensity statistical accuracy better than 2%.

Keywords: Hadron therapy, Beam monitor, Silicon pixel sensor

1. Introduction

The cancer treatment with hadron beams has seen rapid developments in clinical use over the past 10-15 years[1]. Today about 70 proton and carbon-ion therapy centers are in operation all over the world[2]. When a proton or an ion travels in matter, most of its energy is deposited very close to the end of the trajectory. This is called the Bragg-peak mechanism. Because of this the high-dose Bragg peak can be delivered to the tumor by modulating the beam energy. The dose delivered to the surrounding healthy tissue is less compared to X-ray radiation therapy and can be minimized further by varying the incident direction of the ion beam.

A standard hadron therapy facility consists of ion sources, an accelerator to bring the ions to hundreds of MeV/u , and beam delivering systems to transport the ion beam to a clinic and then to the tumor. In the active spot-scanning delivery system, the scanning magnets deflect the pencil beam to the required transverse position and the accelerator modulates the beam energy to deliver the Bragg peak of the beam to the required longitudinal position[3].

To ensure accurate delivery of a prescribed dose to the tumor, the beam monitor system is required to measure the beam's intensity, centroid position and profile in real time. The beam monitor must also have low material budget to reduce the disturbances to the beam.

Currently parallel-plate ionization chambers with one large electrode or electrodes segmented in strips[3, 4, 5, 6] or pixels[6] are commonly used at hadron therapy facilities to monitor the beam online. The ionization chambers can measure the beam with a position resolution sub-millimeter and intensity accuracy about 1% that are the general requirements of hadron therapy[3, 6].

We are developing an online beam monitor that is based on TPC (time projection chamber) detection principle[7]. Eight silicon pixels sensors, *Topmetal-II*⁻ [8], are used as the anode array. This beam monitor measures the position of the beam with a better than 20 μm resolution and the angle of the beam with about 0.5° resolution. These characteristics improve the control of beam and the accuracy of hadron therapy.

In part 2 we describe the silicon pixel charge sensor *Topmetal-II*⁻ and the design of the beam monitor that uses this sensor. We show the measurement results at HIRFL in part 3 and the comparison with the ionization chambers in part 4.

2. Design of the beam monitor

The beam monitor developed for hadron therapy locates at the end of a beam line, in ambient air and at room temperature.

2.1. *Topmetal-II*⁻

Topmetal-II⁻ is a charge sensor, fabricated using a CMOS 0.35 μm technology. The sensor has $72 \times 72 = 5184$ pixels. Each pixel size is about $83 \times 83 \mu\text{m}^2$. This leads to

*Corresponding author

Email addresses: zwang@mails.ccnu.edu.cn (Zhen Wang), sphyl2007@126.com (Xiangming Sun*)

a charge sensitive region of $6 \times 6 \text{ mm}^2$. With the readout circuits the sensor area is $8 \times 9 \text{ mm}^2$.

Each pixel has a $25 \times 25 \text{ }\mu\text{m}^2$ exposed top layer metal pad (hence the name Topmetal), a charge sensitive amplifier (CSA), an analog readout channel and a digital readout channel. The metal pad collects charge. The CSA converts the charge into an analog voltage signal. As we only use the the analog readout of the sensor in the monitor, we will not discuss the digital readout in this paper. In the analog readout, the voltage signal from the CSA goes through two pixel level source-follower stages and then is routed through a chip level analog buffer to be read out. The analog Equivalent Noise Charge (ENC) of the sensor is measured to be below 15 e-. The sensor response to injected charges is linear [9].

2.2. Design of the Monitor

We employ the TPC (time projection chamber) detection principle in our beam monitor design[7]. The TPC detection principle is shown in Fig.1. *Topmetal-II*⁻, being a 2-dimensional pixel charge sensor with readout, is used to collect the ionized negative charges generated by the passing beam. We use air in the volume of the TPC. When the hadron beam passes through the air between the electrodes, electrons and ionized air molecules are generated and start to drift under the influence of the drift potential. The electrons drift towards the *Topmetal-II*⁻ sensor that is connected as the anode of the TPC. These electrons are quickly captured by neutral oxygen or water vapor in the air to form negative ions[10]. It is these negative ions that drift to *Topmetal-II*⁻ and are collected. The slow drift velocity and heavy mass of these ions (compared with electrons) contribute to the improvements in measurement resolution. The slow drift velocity also better matches the shaping time in *Topmetal-II*⁻.

We place two monitors in the beam with the drift field orthogonal to each other. Each monitor provides a 2-dimensional projection of the beam on the anode plane. The beam profile and the incident angle are reconstructed from the two orthogonal projections.

Shown in Fig.1, eight *Topmetal-II*⁻ sensors are lined up to form the anode of the TPC (the monitor). The anode is set to ground, while the cathode, which is 6 cm from the anode, is at -2000 V potential. The field cage is used to make electric field perpendicular to electrodes[11]. The analog readout of the sensor uses a rolling shutter method with a 1.5625 MHz clock. The eight sensors are read out in parallel. The readout time for one frame of the whole monitor is about 3.3 ms.

3. Measurements at HIRFL

We test a monitor in the superficially-placed tumor therapy terminal at the Heavy Ion Research Facility in Lanzhou (HIRFL) China[12]. The scanning magnets in the beam delivery system are shut down and the beam

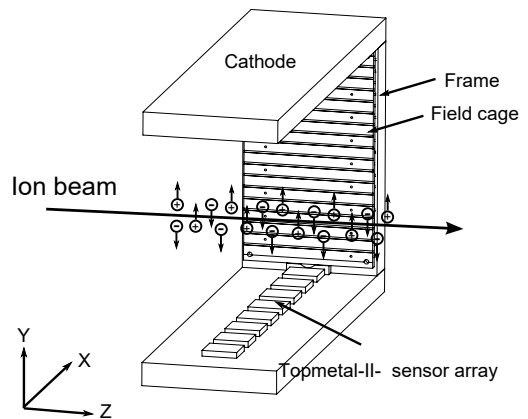


Figure 1: Schematic view of the monitor(The foreground half of the field cage and frame are hid). The eight *Topmetal-II*⁻ sensors are lined as the anode array. The field cage is used to make electric field perpendicular to electrodes. The anode array plane is defined as x-z dimension. The beam passing through the monitor is projected on the x-z dimension.

delivery system delivers a $80.55 \text{ MeV}/u$ carbon ion beam. The beam is time-continuous. The beam passes through a 30 mm long collimator and then the monitor. The collimator has two different inner diameters of 2 mm and 3 mm to choose. Because in the monitor there is a gap of 5.4 mm between each sensor and this gap is the dead area, the position of the monitor is adjusted to make the two-dimensional projection of the beam passing though the collimator right on a single *Topmetal-II*⁻ sensor.

3.1. Two-Dimensional Projection of the Beam

Every 3.3 ms the monitor can provide a two-dimensional projection of the beam. Based on the two-dimensional projection, the monitor can measure position, incident angle and intensity of the beam.

In the test, the carbon ion beam passes through the collimator with a 2 mm inner diameter and then the monitor. The two-dimensional projection of the beam on the monitor is shown in Fig.2. The data is from a single 3.3 ms readout slice. The center of gravity of each row of the two-dimensional projection is calculated by

$$X_{cog} = \frac{\sum_{i=1}^{72} x_i s_i}{\sum_{i=1}^{72} s_i},$$

where s_i is the response of the pixel in i_{th} column and x_i is the coordinate of the pixel in i_{th} column. The centers of gravity from 72 rows are fitted linearly, as the red line in Fig.2 shows. Here, we assume the beam is a straight line and the fitted red line represents the beam. The X of midpoint of the fitted red line is defined as the center position of the beam. The angle between the red line and the positive z-axis is defined as the incident angle of the

beam. The incident angle is about 9° . The sum of the response of all pixels is defined as the intensity of the beam.

In Fig.2 some white bins exist. The corresponding pixels are considered bad pixels. In the above calculation of X_{cog} and beam intensity, these pixels are removed. Besides, the two-dimensional projection of the beam shown in Fig.2 is not smooth, which results from the nonuniformity of pixels. The nonuniformity of pixels means the responses of the pixels are different while the pixels collect the same charges. The nonuniformity of the pixels results from the different decay time constants of the pixels [9]. The CMOS technology is unable to make internal circuit of each pixel identical, which leads to the different decay time constants of the pixels. Bad pixels are the pixels with a too large or small decay time constant. If the decay time constant of one pixel is too large, the pixel would be saturated when continuous charges are collected. Such pixels are called hot pixels. If the decay time constant of one pixel is too small, the response of the pixel would disappear rapidly. Such pixels are called cold pixels. The pixels with a decay time constant less than 3.3 ms are cold pixels. The criteria of distinguishing hot pixels not only depends on the decay time constant of the pixel, but also depends on the collected charges.

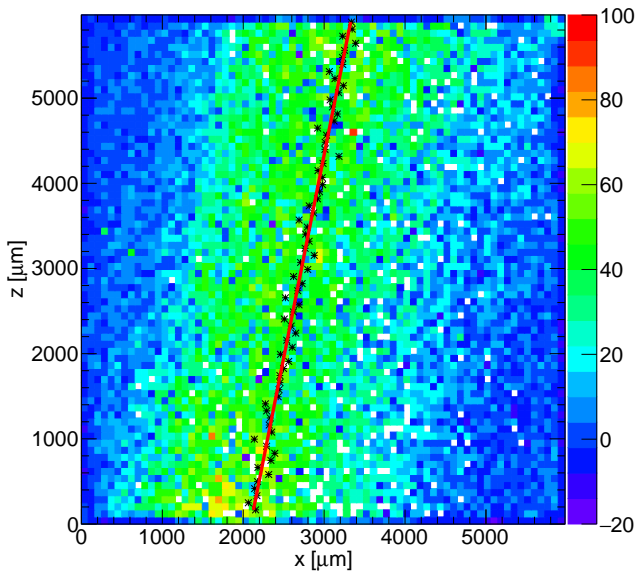


Figure 2: Two-dimensional projection of the 80.55 MeV/u carbon ion beam passing through the collimator with an inner diameter of 2 mm. The black point is the center of gravity of each row. The red line shows the linear fit of the black points. We assume the beam is a straight line and the red line represents the beam. The X of midpoint of the fitted red line is defined as the center position of the beam. The angle between the red line and the positive z-axis is defined as the incident angle of the beam. The incident angle is about 9° . The sum of the response of all pixels is defined as the intensity of the beam. The two-dimensional projection of the beam is not smooth, which results from the nonuniformity of pixels. The white bins are bad pixels with a too large or small decay time constant.

In Fig.3 we show the one-dimensional projection of Fig.2 onto the axis perpendicular to the fitted red line. The Fig.3 shows one-dimensional beam profile.

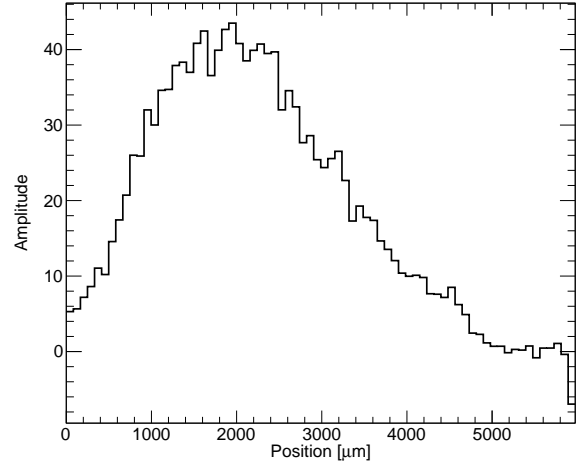


Figure 3: One-dimensional projection of Fig.2 onto the axis perpendicular to the fitted red line.

3.2. Performance of the Monitor

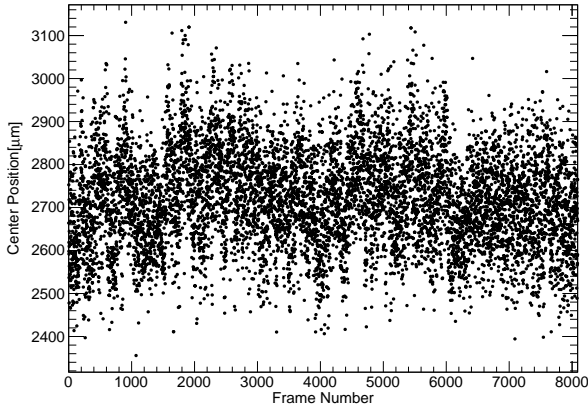
The monitor is designed to measure the fluctuation of the beam position, beam angle and beam intensity. The performance of the monitor is involved in position resolution, angular resolution and intensity accuracy. The performance is studied with a long-time and continuous data acquisition. In this test the beam passes through the collimator with a 3 mm inner diameter and then the monitor in the direction almost parallel to z. The monitor samples 8089 frames during about 26.7 s. The data of 8089 frames is used to show the fluctuation of the beam as a function of time and analyze the position resolution, angular resolution, intensity accuracy of the monitor.

3.2.1. Beam vs Time

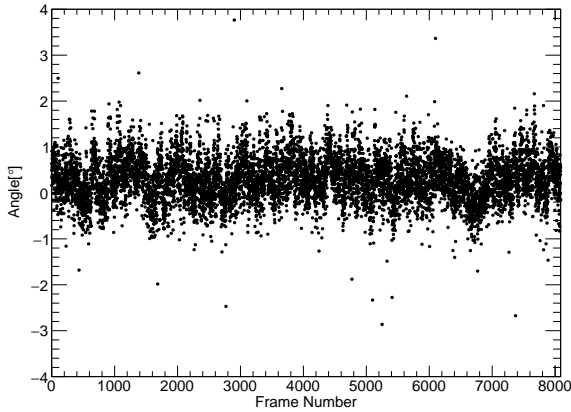
In Fig.4 we show the center position, angle and intensity of the beam as a function of the frame number. One frame represents 3.3 ms.

3.2.2. Position Resolution

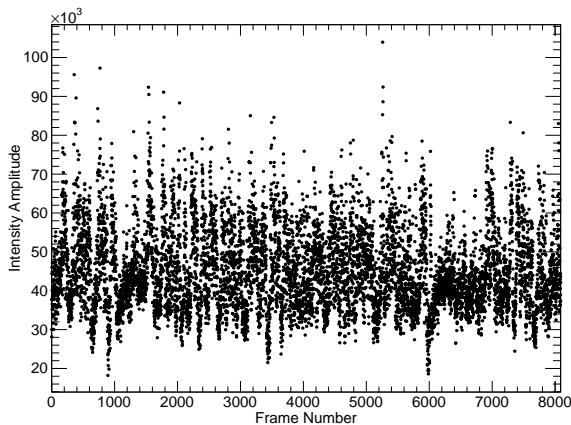
The beam monitor position resolution is a paramount parameter to fulfill the accurate beam delivering. In the test we don't have a calibrated position detector to measure the true position of the beam and the beam itself wobbles slightly. we adapt the following method to calculate the position resolution. We assume the beam is a straight line, the beam doesn't wobble in one frame and the fitted red line from black points of 72 rows represents the beam. The distance vector between the center of gravity (black point) of each row and the fitted red line is defined as delta position. In one frame the delta position of each



(a)



(b)



(c)

Figure 4: Center position, angle and intensity of the beam as a function of the frame number. One frame represents 3.3 ms.

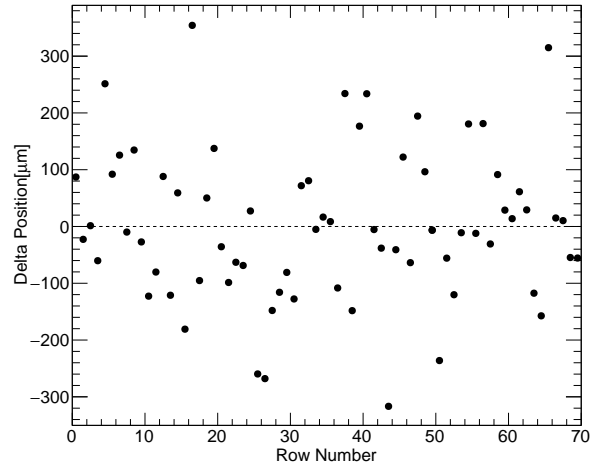


Figure 5: Delta position of each row in one frame. Delta position is the distance vector between the center of gravity (black point) of each row and the fitted red line.

row is shown in Fig.5. The standard error of delta position is defined as position resolution.

In the monitor each frame can give the beam position resolution. The distribution of the position resolution of the 8089 frames is shown in Fig.6. Most probable value of the position resolution is about $17 \mu\text{m}$.

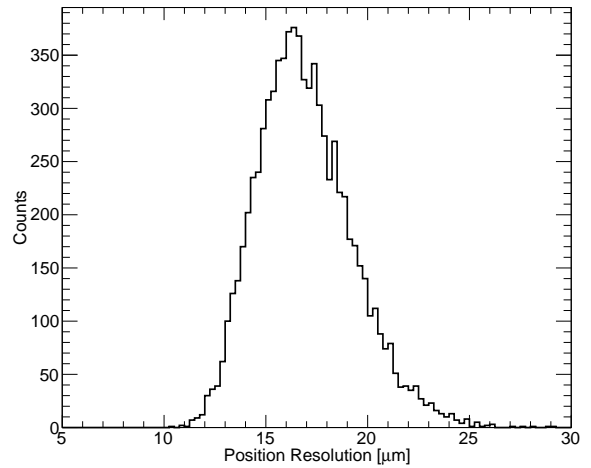


Figure 6: Distribution of the position resolution of the 8089 frames. Most probable value of the position resolution is about $17 \mu\text{m}$.

3.2.3. Angular resolution

The angle between the red line and positive z-axis is defined as the incident angle of the beam. Each frame can give a beam angle. The distribution of the beam angle of the 8089 frames is shown in Fig. 7. The RMS of the distribution of the beam angle is defined as the angular resolution. The angular resolution is about 0.5° partly from the tiny wobble of the beam.

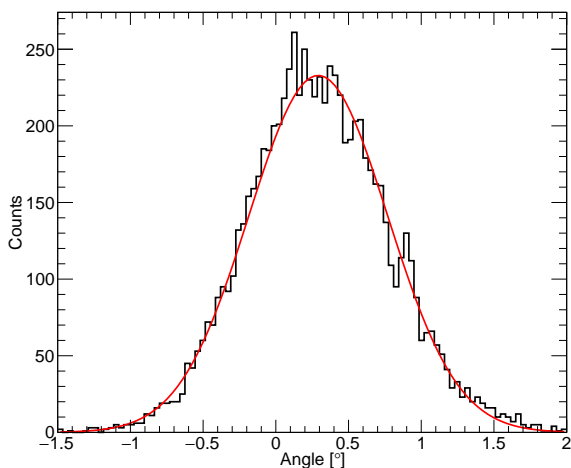


Figure 7: Distribution of the beam angle of the 8089 frames. The angular resolution is about 0.5° partly from the tiny wobble of the beam. The shape is fitted with a Gaussian shape and it is shown here as red curve for eye-directing purpose.

3.2.4. Intensity Accuracy

The dose deposition to the tumor largely depends on the beam intensity. In the test we don't have a calibrated detector to measure the intensity of the beam and the beam from the accelerator is time-varying. we adapt the following method to calculate the intensity accuracy of the monitor. The *Topmetal-II*⁻ contains 72 rows, which is divided into two parts, each part of 36 rows. We assume in one frame the beam doesn't vary and beam intensity in the upper part and lower part is the same. That means the beam is measured twice repeatedly. In one frame, the charges of all the pixels in upper part are summed as Q_{up} and that in the lower part are summed as Q_{down} . $\Delta Q = Q_{up} - Q_{down}$, $Q = (Q_{up} + Q_{down})/2$. The distribution of $\Delta Q/Q$ of the 8089 frames is shown in Fig.8. The mean of the distribution of the $\Delta Q/Q$ approximates zero. The RMS of the distribution of the $\Delta Q/Q$ defined as the beam intensity statistical accuracy is about 1.9%.

4. Comparison with Ionization Chamber

The monitor can provide better than $20 \mu\text{m}$ position resolution and measure the angle of the beam with about 0.5° resolution based on silicon pixel sensor. For those parallel-plate ionization chamber, the mm-scale width of strips restricts the position resolution of that dimension to sub-millimeter.

Besides, in the parallel-plate ionization chamber the ions and electrons are produced along the direction of beam and then move under the electric field almost in parallel with the direction of beams shown in Fig.9. The ions moving along the beam have a significant probability of recombining with the electrons then. With the pencil beam size smaller and intensity higher, the density of ions and elec-

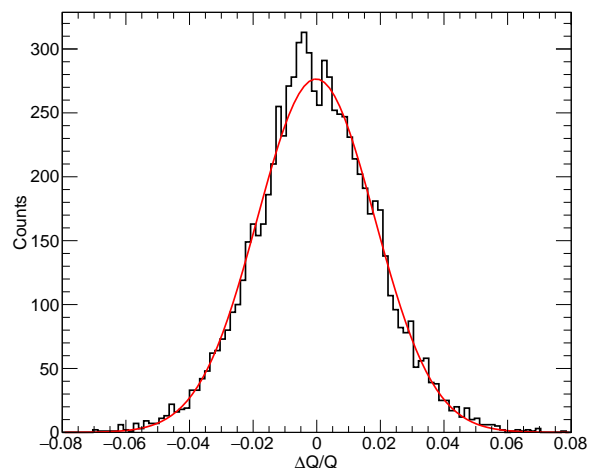


Figure 8: Distribution of $\Delta Q/Q$ of the 8089 frames. Q_{up} is the summation of the charges of all the pixels in upper 36 rows and Q_{down} is the summation of the charges of all the pixels in lower 36 rows in one frame. $\Delta Q = Q_{up} - Q_{down}$, $Q = (Q_{up} + Q_{down})/2$. The mean of the distribution of the $\Delta Q/Q$ approximates zero. The RMS of the distribution is 1.9% which is the beam intensity statistical accuracy. The shape is fitted with a Gaussian shape and it is shown here as red curve for eye-directing purpose.

trons produced along the beam also becomes larger, which results in a higher recombination rate. This signal lost due to recombination will result in inaccurate measurement of beam intensity[10, 13]. On the other hand, for the monitor we are proposing, the ions and electrons produced drift under the electric field which is almost perpendicular to the direction of beam shown in Fig.1. Thus recombination rate of the ions produced at one area with the electrons produced in other area should be less compared to ionization chamber. Therefore, the monitor proposed in this paper contributes to reduce the recombination rate for the sharp pencil beam.

But in the monitor proposed, the nonuniformity of pixels is a main issue.

5. Conclusion and Outlook

The monitor using the silicon pixel sensors *Topmetal-II*⁻ has been developed for online monitoring in hadron therapy. Different from the ionization chamber, the monitor is based on TPC detection principle. The monitor provides better than $20 \mu\text{m}$ position resolution which is higher than current ionization chambers. In principle the monitor contributes to reduce the recombination rate for the sharp pencil beam. Besides, the monitor provides about 0.5° angular resolution.

There is an on-going updated design of this monitor, which includes 2 sets of lined sensor arrays in perpendicular angle. This shall provide 2-dimensional profile of beams injected and passing over both arrays with good resolution in both x-z and y-z dimension. Furthermore, this

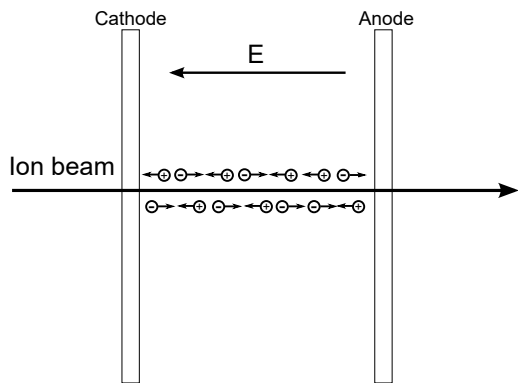


Figure 9: Schematic view of the parallel-plate ionization chamber. The beam passes through the electrodes. The ions and electrons are produced along the direction of beam and then move under the electric field. The ions moving along the beam have a significant probability of recombining with the electrons. This signal lost due to recombination will result in inaccurate measurement of beam intensity.

new design eliminates possible effect of dead area between neighboring sensors, since the array in each dimension contains two lines of eight sensors aligned staggered, such that whenever beam passes over space between sensors in one line, it will be caught by one sensor in the neighboring line.

In the active spot-scanning delivery system, the capability of instantaneous online monitoring of the beam energy is very important. Based on the Lorentz Force, the deflection angles of the ions of different energies are different in the magnet field. We can measure the beam position before and after the magnet field. By comparing the difference of the beam positions before and after the magnet field, we should get the energy profile of the beam. The silicon pixel sensor *Topmetal-II*⁻ with a pixel size of 83 μm is suitable for position sensitive detectors. For the further research we will carry out the principle verification.

Acknowledgments

This work is supported, in part, by the Thousand Talents Program at Central China Normal University and by the National Natural Science Foundation of China under Grant No.11375073, No.11305072, No.1232206 and No.11220101005.

References

[1] G. Kraft, Tumor therapy with heavy charged particles, *Prog Part Nucl Phys* 45, 473 (2000); [http://dx.doi.org/10.1016/S0146-6410\(00\)00112-5](http://dx.doi.org/10.1016/S0146-6410(00)00112-5)
[2] <http://www.ptcog.ch/index.php/facilities-in-operation>
[3] O. Actis, D. Meer and S. Knig, Precise on-line position measurement for particle therapy, *Journal of Instrumentation*, Volume 9, 2014, Pages C12037, <http://stacks.iop.org/1748-0221/9/i=12/a=C12037>

[4] Z. Xu, R. Mao, L. Duan, Q. She, Z. Hu, H. Li, Z. Lu, Q. Zhao, H. Yang, H. Su, C. Lu, R. Hu, J. Zhang, A new multi-strip ionization chamber used as online beam monitor for heavy ion therapy, *Nuclear Instruments and Methods in Physics Research Section A: Accelerators, Spectrometers, Detectors and Associated Equipment*, Volume 729, 21 November 2013, Pages 895-899, ISSN 0168-9002, <http://dx.doi.org/10.1016/j.nima.2013.08.069>.
[5] N. Givehchi, F. Marchetto, A. Boriano, A. Attili, F. Bourhaleb, R. Cirio, G.A.P. Cirrone, G. Cuttone, F. Di Rosa, M. Donetti, M.A. Garella, S. Giordanengo, S. Iliescu, A. La Rosa, P.A. Lojaco, P. Nicotra, C. Peroni, A. Pecka, G. Pitta, L. Raffaele, G. Russo, M.G. Sabini, L.M. Valastro, Online monitor detector for the protontherapy beam at the INFN Laboratori Nazionali del Sud-Catania, *Nuclear Instruments and Methods in Physics Research Section A: Accelerators, Spectrometers, Detectors and Associated Equipment*, Volume 572, Issue 3, 21 March 2007, Pages 1094-1101, ISSN 0168-9002, <http://dx.doi.org/10.1016/j.nima.2006.12.047>.
[6] S. Giordanengo, M. Donetti, M.A. Garella, F. Marchetto, G. Alampi, A. Ansarinejad, V. Monaco, M. Mucchi, I.A. Pecka, C. Peroni, R. Sacchi, M. Scalise, C. Tomba, R. Cirio, Design and characterization of the beam monitor detectors of the Italian National Center of Oncological Hadron-therapy (CNAO), *Nuclear Instruments and Methods in Physics Research Section A: Accelerators, Spectrometers, Detectors and Associated Equipment*, Volume 698, 11 January 2013, Pages 202-207, ISSN 0168-9002, <http://dx.doi.org/10.1016/j.nima.2012.10.004>.
[7] M. Anderson, J. Berkovitz, W. Betts, R. Bossingham, F. Bieser, R. Brown, M. Burks, M. Caldern de la Barca Snchez, D. Cebra, M. Cherney, J. Chrin, W.R. Edwards, V. Ghazikhanian, D. Greiner, M. Gilkes, D. Hardtke, G. Harper, E. Hjort, H. Huang, G. Igo, S. Jacobson, D. Keane, S.R. Klein, G. Koehler, L. Kotchenda, B. Lasiuk, A. Lebedev, J. Lin, M. Lisa, H.S. Matis, J. Nystrand, S. Panitkin, D. Reichold, F. Retiere, I. Sakrejda, K. Schweda, D. Shuman, R. Snellings, N. Stone, B. Stringfellow, J.H. Thomas, T. Trainor, S. Trentalange, R. Wells, C. Whitten, H. Wieman, E. Yamamoto, W. Zhang, The STAR time projection chamber: a unique tool for studying high multiplicity events at RHIC, *Nuclear Instruments and Methods in Physics Research Section A: Accelerators, Spectrometers, Detectors and Associated Equipment*, Volume 499, Issues 23, 1 March 2003, Pages 659-678, ISSN 0168-9002, [http://dx.doi.org/10.1016/S0168-9002\(02\)01964-2](http://dx.doi.org/10.1016/S0168-9002(02)01964-2).
[8] M. An, C. Chen, C. Gao, M. Han, R. Ji, X. Li, Y. Mei, Q. Sun, X. Sun, K. Wang, L. Xiao, P. Yang, W. Zhou, A low-noise CMOS pixel direct charge sensor, *Topmetal-II*, *Nuclear Instruments and Methods in Physics Research Section A: Accelerators, Spectrometers, Detectors and Associated Equipment*, Volume 810, 21 February 2016, Pages 144-150, ISSN 0168-9002, <http://dx.doi.org/10.1016/j.nima.2015.11.153>.
[9] S. Zou, Y. Fan, M. An, C. Chen, G. Huang, J. Liu, H. Pei, X. Sun, P. Yang, D. Wang, L. Xiao, Z. Wang, K. Wang, W. Zhou, Test of Topmetal-II In Liquid Nitrogen For Cryogenic Temperature TPCs, *Nuclear Instruments and Methods in Physics Research Section A: Accelerators, Spectrometers, Detectors and Associated Equipment*, ISSN 0168-9002, <http://dx.doi.org/10.1016/j.nima.2016.05.125>.
[10] G.F. Knoll, *Radiation Detection and Measurement* 3rd edition, 2000, John Wiley and sons Inc., pp.131-132
[11] T. Behnke, K. Dehmelt, R. Diener, L. Steder, T. Matsuda, V. Prael and P. Schade, A lightweight field cage for a large TPC prototype for the ILC, *Journal of Instrumentation*, Volume 5(10), Pages P10011, <http://stacks.iop.org/1748-0221/5/i=10/a=P10011>
[12] Q. Li, Z. Dai, Z. Yan, X. Jin, X. Liu, G. Xiao, Heavy-ion conformal irradiation in the shallow-seated tumor therapy terminal at HIRFL, *Medical & Biological Engineering & Computing*, November 2007, Volume 45, Issue 11, pp 10371043, <http://dx.doi.org/10.1007/s11517-007-0245-3>
[13] T. Hiraoka, K. Kawashima and K. Hoshino, Ion recombination loss in ionization chambers irradiated by proton beams, *The*

British journal of radiology, 1982, 55(656): 585-587.